Sizing the pore of the volume-sensitive anion channel by differential polymer partitioning

Vadim I. Ternovsky[a,b], Yasunobu Okada[a], Ravshan Z. Sabirov[a,*]

[a] *Department of Cell Physiology, National Institute for Physiological Sciences, Okazaki 444-8585, Japan*
[b] *Institute of Cell Biophysics RAS, Pushchino, Moscow Region 142290, Russia*

Received 11 August 2004; revised 15 September 2004; accepted 24 September 2004

Available online 6 October 2004

Edited by Maurice Montal

Abstract Partitioning of ethylene glycol and its polymeric forms into the pore of the volume-sensitive outwardly rectifying (VSOR) anion channel was studied to assess the pore size. Polyethylene glycol (PEG) PEG 200–300 (R_h = 0.27–0.53 nm) effectively suppressed the single-channel currents, whereas PEG 400–4000 (R_h = 0.62–1.91 nm) had little or no effect. Since all the molecules tested effectively decreased electric conductivity of the bulk solution, the observed differential effects between PEG 200–300 and PEG 400–4000 on the VSOR single-channel current are due to their limited partitioning into the channel lumen. The cut-off radius of the VSOR channel pore was assessed to be 0.63 nm.

Keywords: Volume-sensitive anion channel; Pore size; Polymer partitioning; Volume regulation; Osmotic stress

1. Introduction

The volume-sensitive outwardly rectifying (VSOR) anion channel is activated by hypotonic stimulation in most cells studied so far; it mediates osmolyte efflux for regulatory volume decrease (RVD), a vitally important mechanism of cellular homeostasis [1]. Recent studies suggest that this channel also plays a cell-rescuing role by counteracting necrotic cell swelling and even a cell-killing role by inducing apoptotic cell shrinkage [2]. Such versatility of the VSOR channel in its physiological function is related not only to its complex intracellular regulation, but also to its peculiar pattern of permeability: the channel is permeable to inorganic Cl^- ions, intracellular organic molecules (such as glutamate and taurine) and possibly, even ATP^{4-} [3]. However, does the anion channel possess a pore wide enough to be capable of passing all these molecules? To address this question, we systematically studied partitioning of monomeric and polymeric forms of ethylene glycol into the pore of the VSOR channel. Polyethylene glycols (PEGs) obey the viscosity law for random coils in water solutions [4–6] and have been successfully used as tools for pore sizing experiments from single-channel recordings, yielding estimates consistent with X-ray crystallography and electron microscopy data [7,8]. The necessity of employing high concentrations of non-electrolytes, however, has restricted the use of this method to lipid bilayers, and only recently has the method been adopted for patch-clamp studies [9].

2. Materials and methods

2.1. Cells

A human epithelial cell line, Intestine 407, was cultured in Fischer's medium supplemented with 10% newborn bovine serum. For patch-clamp experiments, the cells were grown on glass coverslips coated with 0.1 mg/ml collagen (Nitta Gelatin, Osaka, Japan).

2.2. Solutions

The isotonic Ringer solution contained (mM): 135 NaCl, 5 KCl, 2 $CaCl_2$, 1 $MgCl_2$, 5 Na–HEPES, 6 HEPES, 5 glucose (pH 7.4, 290 mosmol/kg-H_2O). Hypotonic 'high-K^+' bath solution contained (in mM): 100 KCl, 1 $MgCl_2$, 2 $CaCl_2$, 5 Na–HEPES, 6 HEPES, and 5 glucose, pH 7.4 (218 ± 4 mosmol/kg-H_2O). The standard pipette solution contained (in mM): 100 CsCl, 1 $MgCl_2$, 2 $CaCl_2$, and 5 HEPES, pH 7.4, adjusted with CsOH (208 ± 3 mosmol/kg-H_2O). In some experiments, the CsCl concentration was reduced down to 30 mM or Cs^+ ions were replaced with equimolar TEA^+. For polymer partitioning experiments, the non-electrolytes (PEG 3400 from ICN Biomedicals, Aurora, OH, and all others from Wako Pure Chemical, Osaka, Japan) were added to a pre-made standard pipette solution to a final concentration of 20% (wt/vol). The osmolality was measured using a freezing-point depression osmometer (OM802, Vogel, Germany). The conductivity was measured using a B-173 conductivity meter (Horiba, Kyoto, Japan). The hydrodynamic radius (R_h) of triethylene glycol was determined by viscosity measurements as described before [4–6,9]. Other radii were taken from [9].

2.3. Electrophysiology

Patch electrodes were fabricated from borosilicate glass capillaries using a laser micropipette puller (P-2000, Sutter Instrument, Novato, CA). High osmotic pressure generated by the non-electrolytes added into the pipette greatly decreased the stability of patches formed using relatively wide 2–3 MΩ pipettes. However, when the pipette tip was smaller (4–6 MΩ) the patches survived long enough to perform accurate single-channel measurements in the presence of non-electrolytes. The single-channel events rapidly became unstable when the non-electrolytes were added to the intracellular (bath) solution. Therefore, bath application is not studied in the present paper. Membrane currents were measured with an EPC-9 patch-clamp system (Heka-Electronics, Lambrecht/Pfalz, Germany). The membrane potential was controlled by shifting the pipette potential (V_p). The membrane potential is reported as $-V_p$. Currents were filtered at 1 kHz and sampled at 5–10 kHz. Data acquisition and analysis were done using Pulse + PulseFit (Heka-Electronics). Liquid junction potentials were calculated according to [10] and were corrected either on- or off-line

* Corresponding author. Fax: +81-564-55-7735.
E-mail address: sabirov@nips.ac.jp (R.Z. Sabirov).

Abbreviations: VSOR, volume-sensitive outwardly rectifying; PEG, polyethylene glycol

0014-5793/$22.00 © 2004 Published by Elsevier B.V. on behalf of the Federation of European Biochemical Societies.
doi:10.1016/j.febslet.2004.09.051

when appropriate. In all single-channel recordings, the membrane patches were first held at −100 mV for 500 ms to fully activate the volume-sensitive anion channels and then 1000 ms step-pulses were applied to the test potentials as indicated. All experiments were performed at room temperature (23–25 °C).

2.4. Data analysis

Single-channel amplitudes were measured by manually placing a cursor at the open and closed channel levels. The reversal potentials were calculated by fitting *i–V* curves to a second-order polynomial [9]. Data were analyzed in Origin 5–7 (OriginLab Corporation, Northampton, MA). Pooled data are given as means ± S.E.M. of *n* observations. Statistical differences in slopes of linear fits were evaluated by analysis of covariance using StatsDirect software (StatsDirect Ltd, Cheshire, UK) and considered significant at $P < 0.05$.

3. Results and discussion

3.1. Activation of single VSOR channels by cell swelling

Human epithelial Intestine 407 cells are known to respond to a hypotonic stimulation with a robust RVD and activation of a volume-sensitive anion conductance [1]. Cell-attached patches were silent in isotonic conditions. Hypotonic stimulation of cells after giga-ohm seal formation caused very little or no channel activation. In contrast, when cells were swollen in hypotonic high-K^+ solution prior to seal formation for approx. 5–10 min, a high level of single-channel activity was observed in the on-cell mode, as reported previously [11]. The single-channel events displayed outward rectification (Fig. 1A and C, open circles) and were insensitive to the replacement of Cs^+ with TEA^+ in the pipette solution (Fig. 1B and C). Reducing the pipette CsCl concentration from 100 to 30 mM reduced the channel amplitude to 35 ± 1% (Fig. 1B) and caused a positive shift of the reversal potential of 11 ± 3 mV, consistent with anionic selectivity of this channel. Single-channel events displayed profound time-dependent inactivation at large positive potentials (Fig. 1D). Thus, the outward rectification, anion selectivity and time-dependent inactivation reproduce the phenotype of the VSOR anion channels observed earlier in Intestine 407 cells [11,12] and other cell types [13,14].

3.2. Differential effect of polymers on VSOR current amplitudes

When a series of non-electrolytes (ranging from 0.27 to 1.91 nm in radius) were applied from the extracellular side, VSOR single-channel amplitude was altered to different extents (Fig. 2A). The distribution of single-channel amplitudes was fairly narrow in control conditions, but became broader in the presence of non-electrolytes (Fig. 2B). In order to account for this effect, we collected a large number of single-channel events and averaged the amplitudes of the major pools in the amplitude histograms (Fig. 2B). The mean values were then used to construct current-to-voltage relationships at 80–140 mV (Fig. 2C).

Since the *i–V* curves were roughly linear in this range of voltages, the weighted linear fits were used to evaluate the single-channel slope conductances and their standard errors. The relative changes in the single-channel conductance in comparison with the relative changes in the bulk solution conductivity are summarized in Fig. 3A.

All polymers tested efficiently decreased the bulk pipette solution conductivity (Fig. 3A, triangles). However, larger molecules (PEG 400–4000 of $R_h = 0.62$–1.91 nm) had little or no effect on the channel amplitude or the slope conductances, and only ethylene glycol ($R_h = 0.27$ nm), triethylene glycol ($R_h = 0.38$ nm) and PEG of molecular weight 200–300 ($R_h = 0.45$–0.53 nm) effectively suppressed the single-channel outward conductance (Fig. 3A, circles). In accord with previous reports [4–9], this result can be interpreted to mean that only small molecules were able to reach the channel interior, whereas larger polymers were effectively excluded from the

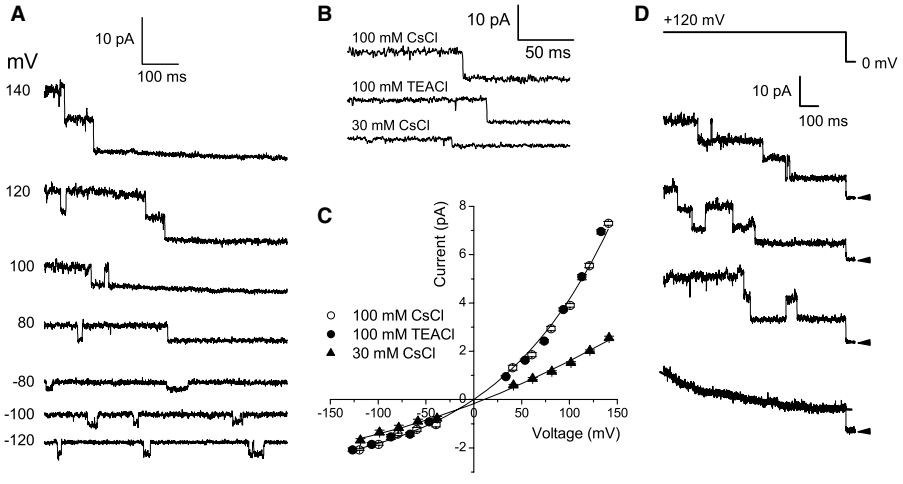

Fig. 1. Single volume-sensitive anion channel currents recorded from cell-attached patches on pre-swollen cells. (A) Representative current traces recorded at different voltages as indicated on the left of each trace. (B) Single-channel current traces recorded at +140 mV with pipette containing 100 mM CsCl (upper trace), 100 mM TEA-Cl (middle trace) and 30 mM CsCl (lower trace). (C) Unitary current–voltage relationship for volume-sensitive anion channel events recorded in the cell-attached mode with standard 100 mM CsCl-pipette solution (open circles), 100 mM TEA–Cl-pipette solution (closed circles) and 30 mM CsCl-pipette solution (filled triangles). Each data point represents the mean ± S.E.M. of 5–62 measurements from 8 to 14 different patches. A larger number of events were observed at high positive potentials, whereas the number of events was less at intermediate voltages due to slower rate of inactivation. (D) Inactivation of single volume-sensitive anion channels at large positive potentials. Three representative traces are shown. The reference null-trace is subtracted. Bottom trace is an ensemble average of 15 records. Solid line represents a single-exponential fit with a time constant of 417 ± 5.7 ms.

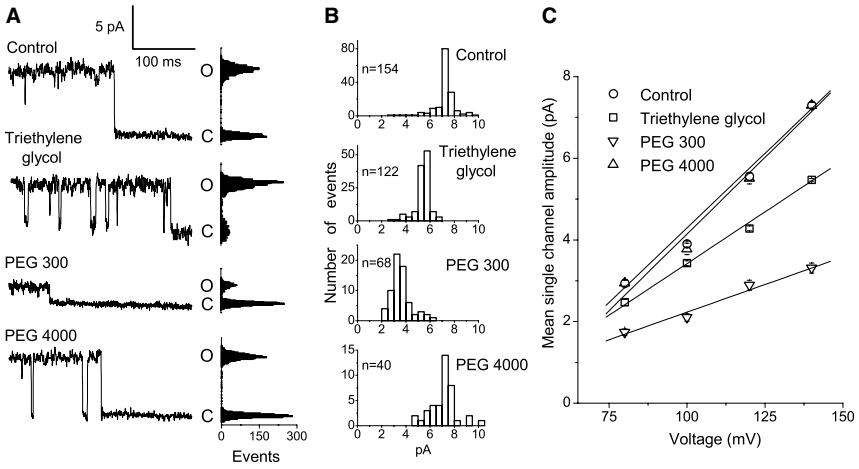

Fig. 2. Effects of non-electrolytes added from the extracellular side on single volume-sensitive anion channel currents. (A) Representative current traces recorded at +140 mV in the absence (upper trace) and in the presence of triethylene glycol, PEG 300 or PEG 4000 (lower traces) in the pipette. The corresponding all-point histograms are shown at the right of each record; "O" and "C" denote open and closed state, respectively. Peak-to-peak single-channel amplitude was 7.6 pA in control conditions, and 5.5, 2.2 and 6.8 pA in the presence of triethylene glycol, PEG 300 and PEG 4000, respectively. (B) Single-channel event amplitude histograms at +140 mV. Single-channel events were collected in control conditions (14 patches) and test conditions in which the pipette solution contained 20% triethylene glycol (13 patches), PEG 300 (11 patches) or PEG 4000 (15 patches). Events of major pools (defined as means ± 3 S.D.) were averaged to yield mean single-channel current and S.E.M. at +140 mV. (C) Single-channel current-voltage relationships. Single-channel events were collected at different potentials and processed as in (B). Solid lines are linear fits with slopes corresponding to the unitary outward conductances of 73.7 ± 1.9, 50.6 ± 1.1, 27.1 ± 3.4 and 73.0 ± 1.6 pS for control, triethylene glycol, PEG 300 and PEG 4000, respectively. Slopes for triethylene glycol and PEG 300 are significantly different from the control slope at $P < 0.05$.

VSOR channel pore. The ability to suppress the VSOR channel conductance was non-monotonic and displayed a profound minimum with PEG 300 ($R_h = 0.53$ nm). This behavior is strikingly different from a previous result we obtained for maxi-anion channel, in which we observed a lower plateau level for small molecules which freely penetrated the channel pore, followed by a rather smooth transition to an upper plateau level for excluded polymers [9]. The relative inhibition of VSOR single-channel conductance by PEG 300 was even greater than the relative decrease in bulk conductivity of PEG 300-containing pipette solution. This would suggest that PEG 300 not only passively partitions between the bulk pipette solution and the channel interior, but also binds to the pore lumen. This binding may increase the effective concentration of the polymer inside the pore, causing the enhanced suppression of ionic transport through the channel. The size of the non-electrolyte is essential to this effect, because PEG 400 ($R_h = 0.62$ nm), which is only slightly larger than PEG 300 (by 0.09 nm in radius), fails to produce such an inhibition. Another process that may affect the size-dependent part of the curve in Fig. 3A is related to the osmotically driven water flow, which may counteract the diffusion of the solutes into the channel and is larger for smaller molecules added at the same weight concentration.

3.3. Dimensions of the VSOR channel

The radii of PEG 300 (0.53 nm) and PEG 400 (0.62 nm) give an approximate estimation of the pore size of the VSOR channel. A more precise way to estimate the VSOR channel pore size from these experiments would be to determine the

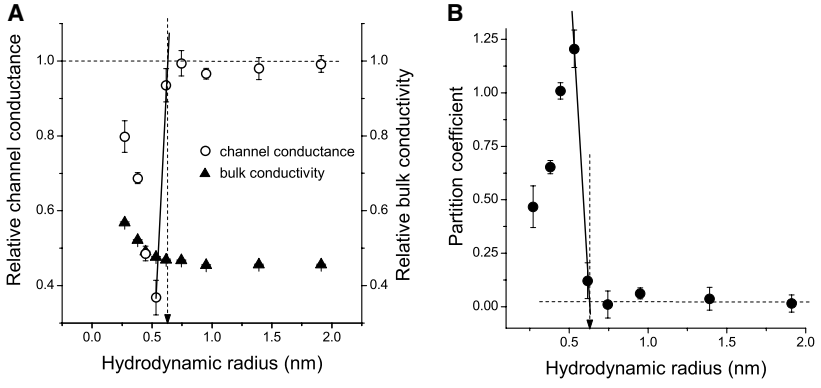

Fig. 3. Effects of polymers on the VSOR single-channel conductance. (A) Relative changes in the unitary single-channel conductance as a function of the hydrodynamic radius (R) of non-electrolyte molecules included in the pipette. Open circles represent the outward slope conductance obtained as in Fig. 2C. Filled triangles represent the relative decrease in the bulk conductivity of the pipette solutions used in these experiments. (B) Partition coefficients calculated according to Eq. (1) as a function of the hydrodynamic radius of non-electrolyte molecules.

cut-off size for the polymers, defining it as a point of intersection between the rising phase of the size-dependent portion of the curve and the size-independent upper plateau level. The point at which the two lines shown in Fig. 3A intersect yields an estimation of the VSOR pore size of 0.63 nm.

The polymer partition coefficient (v) normalizes the change in channel conductance by the change in bulk solution conductivity [5,6,15,16]:

$$v = [(\gamma - \gamma_0)/\gamma_0]/[(\chi - \chi_0)/\chi_0] \quad (1)$$

where γ and χ are the channel conductance and bulk solution conductivity in the presence of non-electrolytes, respectively, and γ_0 and χ_0 are the same parameters in control pipette solution. In the plot of partition coefficient as a function of polymer hydrodynamic radius (Fig. 3B), the descending portion corresponds to a zone of transition from full penetration to complete exclusion. The pore cut-off size of 0.63 nm obtained from this plot is in agreement with the value derived from the analysis of relative channel conductance changes.

3.4. Comparison with other estimates and conclusion

In a previous study [17], analysis of the permeability of the VSOR channel to organic anions of different size yielded a pore radius of 0.37 or 0.58 nm depending on whether or not frictional forces were taken into account. From experiments using calixarenes, basket-shaped compounds that act as permeant blockers of VSOR, the lower and upper limits of 1.1×1.2 and 1.7×1.2 nm, respectively, for the cross-sectional dimensions of the channel pore were determined [18,19]. The minimum and maximum of the pore radius calculated as a geometric mean of these dimensions are 0.57 and 0.71 nm, respectively. The present study is the first attempt to evaluate the size of the VSOR channel pore using non-charged molecules as probes. These three unrelated and totally independent approaches (anion permeation, voltage-dependent block and polymer partitioning) yield a converging estimate of the VSOR pore radius of 0.6–0.7 nm. This value is compatible with the role of the VSOR channel as a mediator of swelling-induced efflux of intracellular osmolytes, including most amino acids with effective radii of approx. 0.3–0.4 nm. Surprisingly, our estimate of the VSOR pore size corresponds very closely to the radius of ATP^{4-} and $MgATP^{2-}$ (about 0.6–0.7 nm [9]). This result is in agreement with the voltage-dependent block of the VSOR channel produced by extracellular ATP [3,12]. Can ATP molecules be translocated through the VSOR channel? Relief of ATP block at large positive voltages supports this idea for aortic endothelial cells [3]. However, the swelling-induced release of ATP from human epithelial Intestine 407 cells was insensitive to the inhibitors of VSOR [20,21], arguing against this possibility. In contrast, our polymer partitioning study of maxi-anion channel (which is also activated by cell swelling and has a larger conductance of ~400 pS) yielded a pore radius of ~1.3 nm, which is clearly larger than the size of ATP^{4-} and $MgATP^{2-}$ [9]. We believe that the maxi-anion channel is best suited to its function as an ATP channel and, where present, serves as the preferred pathway for release of ATP^{4-} and/or $MgATP^{2-}$ [22].

Acknowledgements: This work was supported by Grants-in-Aid for Scientific Research (A) and (C) to Y.O. and R.Z.S. from the MEXT of Japan. The authors thank E.L. Lee for reviewing the manuscript, T. Okayasu for secretarial help as well as M. Ohara and K. Shigemoto for technical support.

References

[1] Okada, Y. (1997) Am. J. Physiol. 273, C755–C789.
[2] Okada, Y., Maeno, E., Shimizu, T., Manabe, K., Mori, S. and Nabekura, T. (2004) Pflugers Arch. 448, 287–295.
[3] Hisadome, K., Koyama, T., Kimura, C., Droogmans, G., Ito, Y. and Oike, M. (2002) J. Gen. Physiol. 119, 511–520.
[4] Sabirov, R., Krasilnikov, O.V., Ternovsky, V.I., Merzliak, P.G. and Muratkhodjaev, J.N. (1991) Biol. Membr. 8, 280–291.
[5] Sabirov, R.Z., Krasilnikov, O.V., Ternovsky, V.I. and Merzliak, P.G. (1993) Gen. Physiol. Biophys. 12, 95–111.
[6] Krasilnikov, O.V., Sabirov, R.Z., Ternovsky, V.I., Merzliak, P.G. and Muratkhodjaev, J.N. (1992) FEMS Microbiol. Immunol. 5, 93–100.
[7] Krasilnikov, O.V. (2002) in: Structure and Dynamics of Confined Polymers (Kasianowicz, J.J., Kellermayer, M.S.Z. and Deamer, D.W., Eds.), pp. 73–91, Kluwer Publisher, Dordrecht, The Neatherlads.
[8] Bezrukov, S.M. and Kasianowicz, J.J. (2002) in: Structure and Dynamics of Confined Polymers (Kasianowicz, J.J., Kellermayer, M.S.Z. and Deamer, D.W., Eds.), pp. 93–106, Kluwer Publisher, Dordrecht, The Neatherlads.
[9] Sabirov, R.Z. and Okada, Y. (2004) Biophys. J. 87, 1672–1685.
[10] Barry, P.H. and Lynch, J.W. (1991) J. Membr. Biol. 121, 101–117.
[11] Okada, Y., Petersen, C.C., Kubo, M., Morishima, S. and Tominaga, M. (1994) Jpn. J. Physiol. 44, 403–409.
[12] Tsumura, T., Oiki, S., Ueda, S., Okuma, M. and Okada, Y. (1996) Am. J. Physiol. 271, C1872–C1878.
[13] Jackson, P.S. and Strange, K. (1995) J. Gen. Physiol. 105, 643–660.
[14] Sabirov, R.Z., Prenen, J., Droogmans, G. and Nilius, B. (2000) J. Membr. Biol. 177, 13–22.
[15] Bezrukov, S.M., Vodyanoy, I., Brutyan, R.A. and Kasianowicz, J.J. (1996) Macromolecules 29, 8517–8522.
[16] Rostovtseva, T.K., Nestorovich, E.M. and Bezrukov, S.M. (2002) Biophys. J. 82, 160–169.
[17] Nilius, B., Voets, T., Eggermont, J. and Droogmans, G. (1999) in: Chloride Channels (Kozlowski, R., Ed.), pp. 47–63, Isis Medical Media Ltd., Oxford, England.
[18] Droogmans, G., Prenen, J., Eggermont, J., Voets, T. and Nilius, B. (1998) Am. J. Physiol. 275, C646–C652.
[19] Droogmans, G., Maertens, C., Prenen, J. and Nilius, B. (1999) Br. J. Pharmacol. 128, 35–40.
[20] Hazama, A., Miwa, A., Miyoshi, T., Shimizu, T. and Okada, Y. (1998) in: Cell Volume Regulation: The Molecular Mechanism and Volume sensing Machinery (Okada, Y., Ed.), pp. 93–98, Elsevier, Amsterdam.
[21] Hazama, A., Shimizu, T., Ando-Akatsuka, Y., Hayashi, S., Tanaka, S., Maeno, E. and Okada, Y. (1999) J. Gen. Physiol. 114, 525–533.
[22] Sabirov, R.Z. and Okada, Y. (2004) Jpn. J. Physiol. 54, 7–14.